BIOCHEMISTRY
including biophysical chemistry & molecular biology

Article

pubs.acs.org/biochemistry

Inhibition of Apurinic/Apyrimidinic Endonuclease I's Redox Activity Revisited

Jun Zhang,[§] Meihua Luo,[‡] Daniela Marasco,[∥] Derek Logsdon,[†] Kaice A. LaFavers,[†] Qiujia Chen,[†] April Reed,[‡] Mark R. Kelley,[‡,†] Michael L. Gross,[§] and Millie M. Georgiadis*[,†,⊥]

[†]Department of Biochemistry and Molecular Biology and [‡]Section of Pediatric Hematology and Oncology, Department of Pediatrics, Indiana University School of Medicine, Indianapolis, Indiana 46202, United States

[§]Department of Chemistry, Washington University in St. Louis, St. Louis, Missouri 63130, United States

[∥]Department of Pharmacy, University of Naples Federico II, Via Mezzocannone, 16, 80134 Naples, Italy

[⊥]Department of Chemistry and Chemical Biology, Purdue School of Science, Indiana University-Purdue University Indianapolis, Indianapolis, Indiana 46202, United States

Supporting Information

ABSTRACT: The essential base excision repair protein, apurinic/apyrimidinic endonuclease 1 (APE1), plays an important role in redox regulation in cells and is currently targeted for the development of cancer therapeutics. One compound that binds APE1 directly is (*E*)-3-[2-(5,6-dimethoxy-3-methyl-1,4-benzoquinonyl)]-2-nonylpropenoic acid (E3330). Here, we revisit the mechanism by which this negatively charged compound interacts with APE1 and inhibits its redox activity. At high concentrations (millimolar), E3330 interacts with two regions in the endonuclease active site of APE1, as mapped by hydrogen−deuterium exchange mass spectrometry. However, this interaction lowers the melting temperature of APE1, which is consistent with a loss of structure in APE1, as measured by both differential scanning fluorimetry and circular dichroism. These results are consistent with other findings that E3330 concentrations of >100 μM are required to inhibit APE1's endonuclease activity. To determine the role of E3330's negatively charged carboxylate in redox inhibition, we converted the carboxylate to an amide by synthesizing (*E*)-2-[(4,5-dimethoxy-2-methyl-3,6-dioxocyclohexa-1,4-dien-1-yl)methylene]-*N*-methoxy-undecanamide (E3330-amide), a novel uncharged derivative. E3330-amide has no effect on the melting temperature of APE1, suggesting that it does not interact with the fully folded protein. However, E3330-amide inhibits APE1's redox activity in *in vitro* electrophoretic mobility shift redox and cell-based transactivation assays, producing IC_{50} values (8.5 and 7 μM) lower than those produced with E3330 (20 and 55 μM, respectively). Thus, E3330's negatively charged carboxylate is not required for redox inhibition. Collectively, our results provide additional support for a mechanism of redox inhibition involving interaction of E3330 or E3330-amide with partially unfolded APE1.

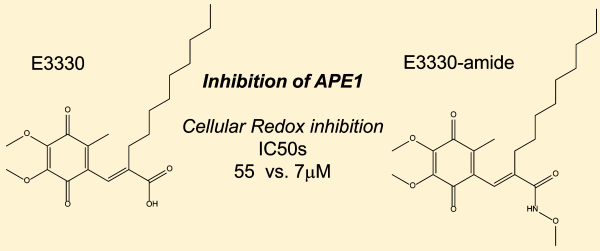

Apurinic/apyrimidinic endonuclease 1 (APE1) plays an important role in the cellular response to oxidative stress by maintaining genomic integrity and regulating redox signaling.[1,2] Upregulation of APE1 in cancer cells is associated with resistance to chemotherapeutic agents,[3−5] while loss of APE1 expression results in the arrest of cell growth, apoptosis,[6] and impairment of mitochondrial function.[7,8] Thus, APE1 is emerging as a potential cancer therapeutic target.[9,10] Activities reported for APE1 include endonuclease activity essential for base excision repair,[11] redox activity that regulates the DNA binding activity of a number of important transcription factors,[12] transcriptional repressor activity through indirect binding to Ca^{2+} responsive elements,[13] and most recently cleavage of RNA-containing abasic sites.[14] Transcription factors that are regulated by APE1's redox activity include AP-1, NF-κB, Erg-1, HIF-1α, p53, PAX, and others.[12,15−21] Currently, efforts to develop novel cancer therapeutics target either the endonuclease (repair) or the redox function of APE1.[10,22]

APE1 was first reported as the redox factor responsible for reducing cellular Jun (c-Jun), thereby increasing its affinity for DNA.[12] Subsequently, many other transcription factors were shown to be redox-regulated by APE1.[12,15−21] Three cysteine residues, C65, C93, and C99, in APE1 are necessary and sufficient for redox activity.[23] Of these residues, C65 and C93 are buried, whereas C99 is solvent-accessible. Further regulation of APE1's activity under conditions of oxidative stress occurs through glutathionylation of C99, which inhibits both DNA binding and endonuclease activity.[24] Oxidation of APE1 also results in a specific disulfide bond formation cascade, implicating C65 as the nucleophilic Cys.[23] This result is consistent with earlier results in which C65 was shown to play an important role in APE1's redox activity.[25] Through analysis

Received: February 12, 2013
Revised: April 4, 2013
Published: April 18, 2013

   dx.doi.org/10.1021/bi400179m | *Biochemistry* 2013, 52, 2955−2966

of single cysteine-to-alanine substitutions in APE1 for each of the seven cysteines, the C65A substitution was identified as the only redox-inactive substitution.[25] Redox activity associated with APE1 is found only in mammals; zebrafish APE contains five of the seven cysteine residues present in the human enzyme in structurally equivalent positions but still lacks redox activity. However, substitution of threonine 58, the zebrafish residue equivalent to C65, with cysteine confers redox activity in both *in vitro* and cell-based redox assays.[26] More recently, APE1's redox function and specifically C65 have been implicated in mediating localization of APE1 to the mitochondria and controlling cell proliferation.[27]

Other approaches to providing mechanistic details concerning APE1's redox activity used a redox inhibitor (*E*)-3-[2-(5,6-dimethoxy-3-methyl-1,4-benzoquinonyl)]-2-nonylpropenoic acid (E3330). E3330 was first reported to bind APE1 with a K_d of 1.6×10^{-9} M,[28] which later studies find to be far too small.[29,30] As the redox activity of APE1 represents a unique target, E3330 has been evaluated for its potential as a chemotherapeutic agent, making the nature of the interaction of E3330 with APE1 of considerable interest and the subject of two recent biophysical studies.

In one of those studies that examined the binding of APE1 and E3330, we reported that E3330 interacts with a partially unfolded form of APE1, as monitored by NEM footprinting and mass spectrometry.[29] Incubating APE1 in the absence of E3330, we found NEM modification of the two solvent-accessible Cys residues, C99 and C138. Over 24 h at room temperature, barely detectable labeling of buried Cys residues was observed. However, in the presence of E3330, 60% of the enzyme had all seven Cys residues labeled with NEM in the same time frame. This result suggests that E3330 interacts with a partially unfolded state of APE1 long enough for the reaction of Cys and NEM to occur. Other evidence of APE1 unfolding that is essential for function includes the finding that localization of APE1 to mitochondria involves exposure of the C-terminal residues 289−318, which serve as the mitochondrial targeting sequence.[31] This exposure would necessarily involve unfolding of the protein structure as it forms an integral part of the protein structure.

In another recent study, nuclear magnetic resonance (NMR) was used to define interactions of E3330 with APE1. In this study, several residues in the proximity of the repair active site of the enzyme showed backbone perturbations consistent with an interaction of E3330 and APE1, specifically at G231, M270, M271, N272, A273, V278, W280, and D308. However, the K_d reported for this interaction, 390 μM at room temperature, indicates the binding affinity is very weak. A mechanism for redox inhibition was then proposed in which E3330 binds specifically to the repair active site of APE1, preventing a conformational change of the protein required for its redox activity.[30] This is a surprising conclusion given that high concentrations of E3330 are required to inhibit the enzyme's endonuclease activity, even as determined by this group who found that significant inhibition was observed at 100 μM but did not report an IC_{50},[30] whereas much lower concentrations are required to inhibit APE1's redox activity. Thus, this study [30] concluded that E3330 acts as a redox inhibitor by binding to the repair active site, thereby stabilizing APE1's structure and preventing it from unfolding. In this scenario, there is no proposed role for E3330's quinone group, known to be critical for redox inhibition. We concluded that E3330 shifts the equilibrium between folded and unfolded states of APE1 toward unfolded states and inhibits the redox activity through direct interaction with the critical redox residue, Cys65, exposed in a partially unfolded state of the protein leading to its inactivation by disulfide bond formation.[29]

In an effort to resolve the disagreement, we pursued additional experimental approaches to determine the nature of the interaction of E3330 with APE1 and report here new insights into the inhibition mechanism. We sought to answer the following key questions. Does E3330 bind specifically to a single site within the repair active site of APE1? Does the interaction of E3330 with APE1 stabilize its structure and thereby prevent a conformational change required for its redox activity? Finally, is the negatively charged carboxylate group of E3330 required for redox inhibition?

EXPERIMENTAL PROCEDURES

Preparation of APE1 Proteins. Full-length human APE1 (APE1) was expressed and purified as previously described.[29] In brief, the protein was expressed as an N-terminal hexa-His SUMO fusion protein. Following lysis using a French press, the crude extract was bound to a Ni-NTA column, and APE1 was released by cleavage with the SUMO-specific Ulp1 protease. The protein was then subjected to SP-Sepharose ion exchange and gel filtration (Superdex 75) chromatographic purification steps.

Hydrogen−Deuterium Exchange (HDX) Mass Spectrometry. Differential, solution-phase HDX experiments were performed to detect conformational changes in full-length APE1 induced by E3330 binding as previously described.[32] A solution of 25 μM full-length APE1 was incubated with 16 mM E3330 for at least 1 h on ice before HDX analysis. Each exchange reaction was initiated by incubating 2 μL of 25 μM protein complex (with or without E3330) with 18 μL of D_2O protein buffer for a predetermined time (10, 30, 60, 120, 900, 3600, and 14400 s) at 4 °C. The final protein concentration was 2.5 μM, and the E3330 concentration was 1.6 mM after D_2O dilution. These conditions resulted in 80% of the protein forming a complex, accepting that the K_d is 390 μM, as measured by NMR.[30] We quenched the exchange reaction by mixing the sample with 30 μL of 3 M urea and 1% TFA at 1 °C. The mixture was passed across a custom-packed pepsin column (2 mm × 2 cm) at a rate of 200 μL/min, and the digested peptides were captured on a 2 mm × 10 mm C_8 trap column (Agilent) and desalted (total time for digestion and desalting of 3 min). Peptides were then separated across a 1.0 mm × 50 mm C_{18} column (1.9 μ Hypersil Gold, Thermo Scientific) with a linear gradient of 4 to 40% CH_3CN and 0.1% formic acid, over 5 min. Protein digestion and peptide separation were conducted on columns immersed in an ice−water bath to reduce the extent of D−H back exchange. Mass spectrometric analyses were conducted at a capillary temperature at 225 °C, and data were acquired at a measured mass resolving power of 100000 at m/z 400. Duplicates were performed for each on-exchange time point.

Peptide Identification and HDX Data Processing. MS/MS experiments were performed with a LTQ Orbitrap mass spectrometer (ThermoFisher, Waltham, MA). Product ion spectra were acquired in a data-dependent mode, and the six most abundant ions were selected for product ion analysis. The MS/MS *.raw data files were converted to *.mgf files and then submitted to Mascot (Matrix Science, London, U.K.) for peptide identification. Peptides included in the peptide set used for HDX had a MASCOT score of ≥20. The MS/MS

Scheme 1. Conversion of E3330 to E3330-amide, (*E*)-2-[(4,5-Dimethoxy-2-methyl-3,6-dioxocyclohexa-1,4-dien-1-yl)methylene]-*N*-methoxy-undecanamide

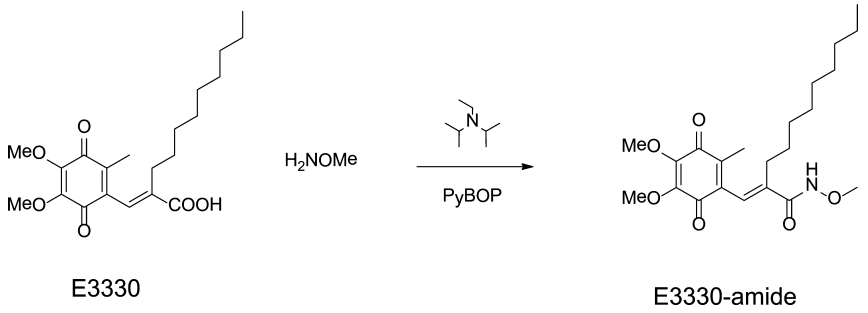

MASCOT search was also performed against a decoy (reverse) sequence, and ambiguous identifications were ruled out. The product ion spectra of all of the peptide ions from the MASCOT search were further manually inspected, and only those that could be verified were used in the coverage.

Differential Scanning Fluorimetry (DSF). DSF assays were performed using a Roche Light Cycler 480 (Roche Applied Science, Indianapolis, IN) with an excitation wavelength of 483 nm and emission of 568 nm. Reactions were conducted in 100 mM HEPES (pH 7.0), 150 mM NaCl, and 4× SYPRO orange (Invitrogen catalog no. S6651) with 0.08% dimethyl sulfoxide (DMSO). Each reaction mixture contained a final protein concentration of 2 μM. E3330 was dissolved in DMSO or absolute ethanol to give final solvent concentrations of 2%, not including DMSO from the SYPRO dye. Titrations of APE1 with E3330 (10 μM to 1 mM) or (*E*)-2-[(4,5-dimethoxy-2-methyl-3,6-dioxocyclohexa-1,4-dien-1-yl)methylene]-*N*-methoxy-undecanamide (E3330-amide) (16 μM to 4 mM) were performed in the presence and absence of 1 mM $MgCl_2$. Titrations of APE1 with Mg^{2+} alone were performed by using a $MgCl_2$ concentration range from 10 μM to 10 mM. SYPRO orange was added after a 15 min incubation with all other reagents. Reaction mixtures were subsequently covered prior to measurements being taken.

Circular Dichroism (CD). Far-UV CD spectra were recorded on a Jasco J-810 spectropolarimeter (JASCO Corp., Easton, MD) in a 225−260 nm interval. Experiments were performed employing a protein concentration of 5.0 μM in 10 mM phosphate buffer (pH 7.0) in the absence and presence of E3330 at 500 μM (1% DMSO), using a 0.1 cm path-length cuvette. Thermal denaturation profiles were obtained by measuring the temperature dependence of the signal at 230 nm in the range of 20−80 °C with a resolution of 0.5 °C and a 1.0 nm bandwidth. A Peltier temperature controller was used to set up the temperature of the sample; the heating rate was 1 °C/min. Data were collected at 0.2 nm resolution with a 20 nm/minute scan speed and a 4 s response and were reported as the unfolded fraction versus temperature.

Synthesis of E3330 and E3330-amide. Both E3330 and E3330-amide were synthesized by the University of Michigan Vahlteich Medicinal Chemistry Core Facility (H. Showalter). E3330 was synthesized as previously described.[33] The synthesis of E3330-amide is shown in Scheme 1.

General Chemical Methods. ^{1}H NMR spectra were recorded on a Bruker 500 MHz spectrometer (Bruker BioSpin Corporation, Billerica, MA). Chemical shifts are reported in δ (parts per million), by reference to the hydrogen residues of a deuterated solvent as the internal standard ($CDCl_3$, δ 7.28; CD_3OD, δ 3.31). Signals were described as s, d, t, and m for singlet, doublet, triplet, and multiplet, respectively. Coupling constants (J) are given in hertz. Mass spectra for compound characterization were recorded on a Micromass LCT time-of-flight instrument (Micromass, Milford, MA) utilizing the electrospray ionization mode. Reactions were monitored by thin-layer chromatography (TLC) using precoated silica gel 60 F254 plates. Chromatography was performed using bulk silica gel F60 (43−60 μm). Reagents and monomers were purchased from common vendors and were used without purification. Glassware was oven-dried before being used for reactions conducted under anhydrous conditions.

(*E*)-2-[(4,5-Dimethoxy-2-methyl-3,6-dioxocyclohexa-1,4-dien-1-yl)methylene]-*N*-methoxy-undecanamide (E3330-amide). Benzotriazol-1-yl-oxytripyrrolidinophosphonium hexafluorophosphate (2.48 g, 4.76 mmol) was added to a stirred solution of (*E*)-2-[(4,5-dimethoxy-2-methyl-3,6-dioxocyclohexa-1,4-dien-1-yl)methylene]undecanoic acid (1.2 g, 3.17 mmol), *O*-methylhydroxylamine hydrochloride (0.34 g, 4.12 mmol), and diisopropylethylamine (1.02 g, 7.93 mmol) in dichloromethane (10.5 mL) under N_2 at room temperature. A mild exotherm was noted, and a clear red solution resulted. After 22 h, TLC (60:50:1 hexane/ethyl acetate/acetic acid) indicated that the reaction was complete. The mixture was diluted with more dichloromethane, washed with water and then saturated brine, and then dried over magnesium sulfate. The solvent was removed *in vacuo*, leaving a red syrup. Chromatography on a column of silica gel under pressure, eluting with a 60:50:1 hexane/ethyl acetate/acetic acid mixture, afforded the pure product as a thick, clear, blood-red syrup (1.0 g, 77%): ESI-MS m/z 408 $[M + H]^+$ and 430 $[M + Na]^+$; ^{1}H NMR (500 MHz, $CDCl_3$) δ 6.49 (s, 1H), 4.06 (s, 3H), 4.02 (s, 3H), 3.87 (s, 3H), 2.13 (t, J = 10.5, 2H), 1.97 (s, 3H), 1.38 (m, 2H), 1.32−1.15 (m, 14H), 0.88 (t, J = 7.1, 3H).

Electrophoretic Mobility Shift Assays (EMSAs). E3330 or E3330-amide was preincubated with 2 μL of purified APE1 (reduced with 1.0 mM DTT for 10 min and then diluted to a concentration of 0.06 mM with 0.2 mM DTT in PBS) in an EMSA reaction buffer that consisted of 10 mM Tris (pH 7.5), 50 mM NaCl, 1 mM $MgCl_2$, 1 mM EDTA, and 5% (v/v) glycerol in a total volume of 16 μL for 30 min. The EMSA was performed as previously described.[23,33]

Transactivation Assays. Panc1 cells (three) with the pGreenFire-NFκB gene (luciferase gene with the NFκB-responsive promoter) stably inserted were treated with increasing amounts of E3330 or E3330-amide, and activity was assayed at 40 h. The cells were lysed, and the *Firefly* luciferase activities were assayed as previously described.[33] The luciferase activity was normalized to the total cell number measured by the MTT assay. All of the experiments were

dx.doi.org/10.1021/bi400179m | *Biochemistry* 2013, 52, 2955−2966

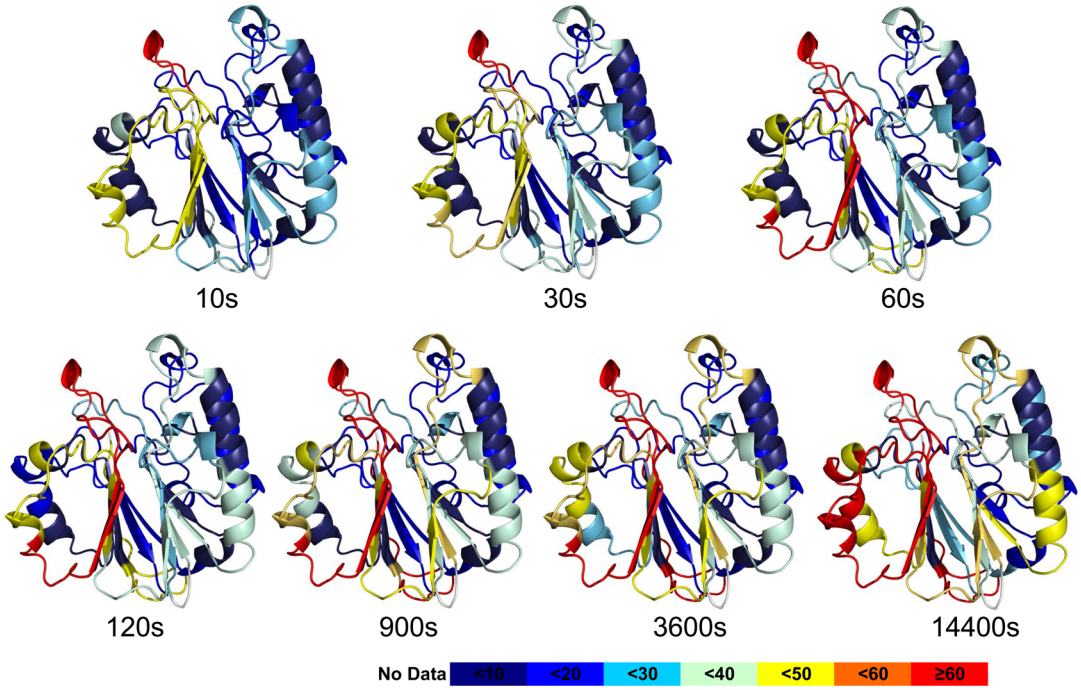

Figure 1. HDX data mapped on the structure of APE1 that are consistent with a fully folded protein. The percentage of deuterium uptake for peptides derived from APE1 at different time points is color-coded on a ribbon rendering of the crystal structure of human APE1 (Protein Data Bank entry 1BIX). The color code indicates the deuterium uptake level: red for regions that exchange very rapidly and dark blue for regions that exchange very slowly. For the most rapidly exchanging peptides, 266−271 and 267−273, more than 70% of the backbone amide hydrogens exchanged with deuterium within 10 s. This region was also identified as interacting with E3330.

performed in triplicate and repeated at least three times in independent experiments.

Cell Survival and Growth Assays. A 3-(4,5-dimethylthiazol-2-yl)-5-(3-carboxymethoxyphenyl)-2-(4-sulfophenyl)-2*H*-tetrazolium (MTT) dye assay for cell growth was performed as previously described.[34,35]

Oligonucleotide Gel-Based APE1 Endonuclease Activity Assays. Oligonucleotide gel-based APE1 endonuclease activity assays were performed as previously described with the following modifications.[36,37] Purified APE1 was incubated with increasing amounts of E3330 in a total volume of 9 μL of assay buffer [5 mM HEPES, 5 mM KCl, 1 mM $MgCl_2$, 0.1% BSA, and 0.005% Triton X-100 (pH 7.5)] at room temperature for 30 min, 1 h, or 2 h. One microliter or 0.2 pmol of 5′-hexachlorofluorescein phosphoramidite (HEX)-labeled tetrahydrofuranyl (THF) oligo [the 26 bp oligonucleotide substrate containing a single THF reside in the middle, yielding a HEX-labeled 14-mer fragment (upon repair)] was added to the mixture, and the mixture incubated for 15 min at 37 °C. The reactions were terminated by adding 10 μL of formamide. Samples (10 μL) were then applied to a 20% polyacrylamide gel containing 7 M urea in 1× TBE buffer at 300 V for 30 min. The amounts of 14-mer to 26-mer products detected were quantitated by using the Hitachi FMBio II Fluorescence Imaging System (Hitachi Genetic Systems, South San Francisco, CA).[36,37]

Fluorescence-Based Kinetic Endonuclease Activity Assays. Compounds E3330 and E3330-amide were tested with an assay for their ability to inhibit APE1 repair function in a plate-based, high-throughput screening (HTS) assay as previously described.[38] A pair of oligonucleotides (Eurogentec, Ltd., Freemont, CA), one containing a 6-FAM fluorescein label at its 5′ end and the second containing a 3′ Dabcyl quencher and an internal tetrahydrofuran (THF) as an abasic (AP) site mimic, with complementary bases was annealed as described previously.[38] Cleavage at the THF site resulted in the release of a 6-FAM-labeled oligonucleotide, which now fluoresced. The increased rate of fluorescence was directly correlated to the amount of APE1 repair activity. Inhibition resulted in a decrease in the rate of fluorescence over time. The assay was performed on an Ultra384 plate reader (Tecan, Durham, NC) in the Chemical Genomics Core Facility at the Indiana University School of Medicine in a 96-well plate for three cycles of 1 min each at 37 °C. A master mix of HTS buffer [50 mM Tris-HCl (pH 8), 50 mM NaCl, 1 mM $MgCl_2$, and 2 mM DTT], water, and annealed oligonucleotide (final concentration of 50 nM) was made, and 100 μL was added to each well. A pretest was performed using 100 μL of the master mix, 50 μL of water, and 50 μL of purified human APE1 protein at various concentrations to test for a linear rate of reaction (data not shown). E3330 and E3330-amide were then diluted 20-fold to the final concentration desired. All dilutions had the vehicle control, DMSO, in equal amounts (final concentration of 0.1%). Then 10 μL of the 20-fold diluted compounds was plated with the master mix in triplicate along with 40 μL of water. APE1 (50 μL of a 0.04 nM solution) was added to the wells, and the solution was immediately assayed. The rate of reaction for each well was normalized to DMSO-only controls and plotted as percent inhibition versus time.

RESULTS

Identification of E3330-Interacting Regions on APE1 by HDX and MS. In light of the reported weak binding (K_d of 390 μM),[30] we performed an HDX analysis with full-length APE1 by using 1.6 mM E3330. This condition should result in approximately 80% complex formation, and indeed, we do find

dx.doi.org/10.1021/bi400179m | *Biochemistry* 2013, 52, 2955−2966

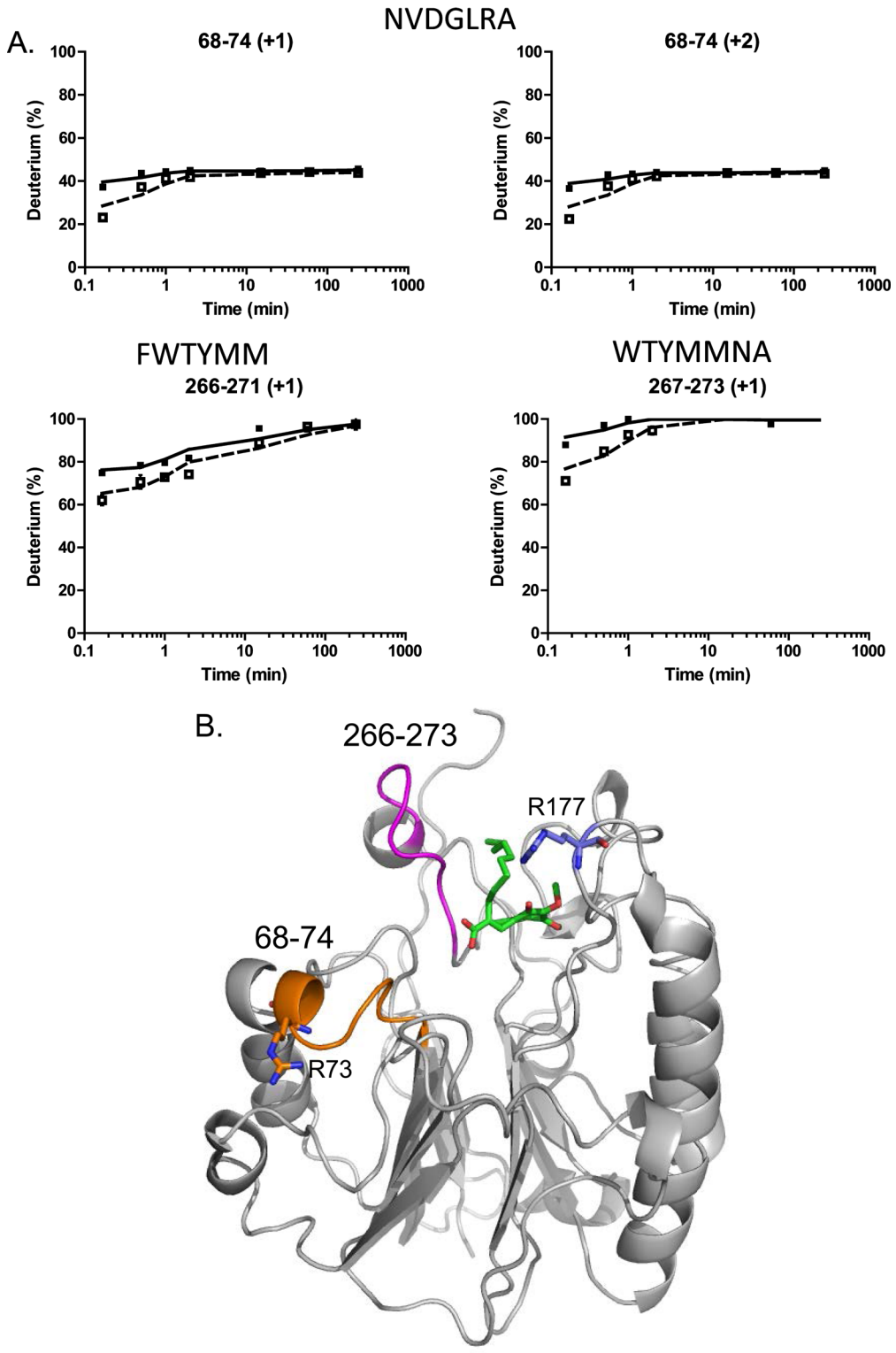

Figure 2. Interaction of E3330 with APE1 as detected by HDX mass spectrometry. (A) HDX data are shown for peptides with slower exchange rates in the presence of 1.6 mM E3330 (□) as compared to the exchange rates in the absence of compound (■). (B) The peptides that showed protection from deuterium exchange are shown highlighted on the structure of APE1. Residues 68−74 are colored orange and residues 266−273 magenta. Colored green is a stick model of E3330 docked in the repair active site with its hydrocarbon tail in the proximity of peptide 266−273. Shown as stick models are R73 (orange) and R177 (blue), two Arg residues in the proximity of the regions of interaction identified by HDX mass spectrometry.

detectable differences in the HDX patterns for an experiment conducted at 4 °C. HDX probes perturbations in the backbone of the protein, quite analogous to the changes monitored by NMR. The backbone perturbations are accompanied by changes in H bonding caused by changes in protein dynamics. The interactions of small molecules such as E3330 with APE1 change the dynamics and allow the interaction sites to be determined. The level of peptide coverage for the experiment

dx.doi.org/10.1021/bi400179m | *Biochemistry* 2013, 52, 2955−2966

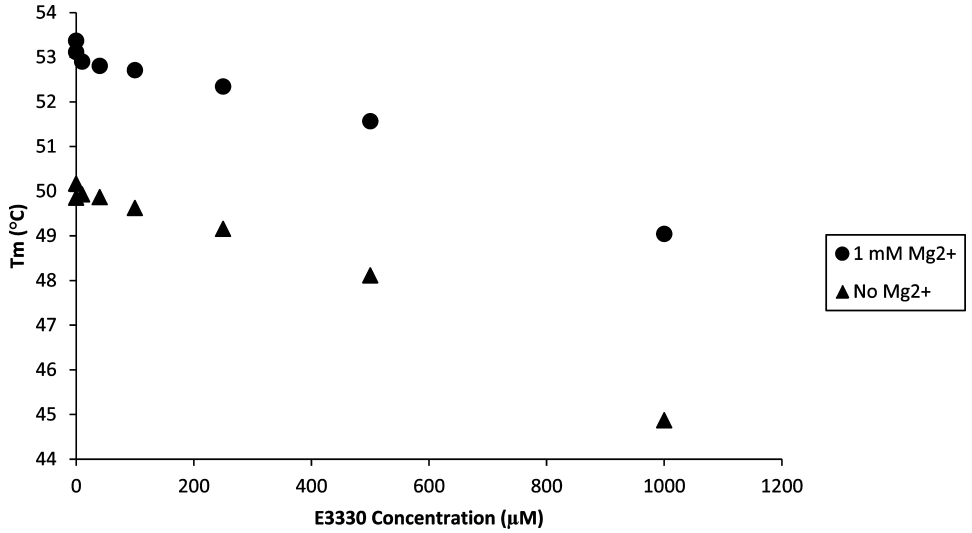

Figure 3. Effect of E3330 on APE1's melting temperature in the presence and absence of Mg^{2+} as measured by DSF. APE1 was titrated with increasing concentrations of E3330 dissolved in DMSO (10 μM to 1 mM) in the presence and absence of 1 mM Mg^{2+}. SYPRO orange dye was then added, and T_m measurements were taken by DSF. The resulting T_m of APE1 was plotted vs the concentration of E3330 in the presence or absence of 1 mM Mg^{2+}. Increasing concentrations of E3330 resulted in decreased APE1 melting temperatures in the presence and absence of Mg^{2+}.

was greater than 90%, allowing us to fully assess the folded state of the protein and the effect of added E3330, as is discussed in the following paragraph.

The dynamics of full-length APE1 in the absence of E3330 is in agreement with reported crystal structures[39,40] (Figure 1): the less structured and exposed regions exhibit relatively fast exchange with deuterium, whereas structured and buried regions of the protein exchange slowly. The most rapidly exchanging regions are represented by peptides 266−271 and 267−273 in which more than 70% of the backbone amide hydrogens exchanged with deuterium within 10 s (Figure 1 and Figure S1 of the Supporting Information). This region is a highly exposed loop on the surface of the protein near the repair active site. On the other hand, regions within the hydrophobic core (residues 63−72, 83−93, 183−191, 208−216, and 285−297) are highly protected from exchange, and they underwent <10% exchange even after incubation for 1 h. One region of intermediate exchange contains residues 93−134. These residues make up the terminal strand and half of each of the next two strands on the end of one β sheet that comprises half of APE1's β sandwich fold along with an intervening α-helical element. This region also includes two of the three Cys residues, C93 and C99, which are critical for APE1's redox activity.

The peptides for which changes in deuterium uptake were observed in the presence of E3330 include 68−74 (seen for both the singly and doubly charged peptides), 266−271, and 267−273 representing two distinct regions in the protein (Figure 2 and Figure S1 of the Supporting Information). For all of these observed peptides, the largest differences in deuterium uptake were observed for the 10 s time point and persisted for at most 10 min. The samples treated with E3330 showed a decreased level of deuterium uptake for a few peptides as compared to the control sample, indicative of protection from exchange. Peptides 266−271 and 267−273 include several of the residues identified in the NMR study (M270, M271, N272, and A273) as interacting with E3330. Thus, our results confirm some of the interaction of E3330 as identified in the NMR study. However, the second peptide identified in our HDX studies (68−74) was not identified as a region of interaction by NMR.

We also have HDX results when E3330 was incubated with an N-terminally truncated version of APE1 (Δ40 APE1) at a decreased concentration of 25 μM (see the Supporting Information). Now we estimate approximately 8% complex formation, considering the equilibrium expression. We might expect that the same peptides, 68−74, 270−284, and 272−284, should show differences in HDX at the lower, 25 μM E3330 concentration, but the changes would be smaller because complex formation is attenuated by a factor of 10. We are still able to detect changes over the same regions of the protein as those identified for the experiment at a higher (1.6 mM) E3330 concentration (Figure S2 of the Supporting Information). This demonstrates that HDX is sufficiently sensitive to report on a small amount (<10%) of complex formation, although admittedly this would be difficult to assign in the absence of the results for the 1.6 mM E3330 experiment in which 80% complex formation is predicted. A second finding from this experiment was that the N-terminal region of APE1 does not affect the interactions of E3330 with APE1.

Effect of E3330 on the Melting Temperature of APE1. To further assess the binding interaction of APE1 with E3330, differential scanning fluorimetry (DSF) and circular dichroism assays were performed. The DSF assay relies on the fluorescence of SYPRO orange to report on the folded state of the protein as the temperature is increased.[41] The melting temperature of full-length APE1 as measured in this assay was 52 °C. First, we examined the effect of the catalytically important Mg^{2+} on the melting temperature of APE1. Titration with Mg^{2+} increased the melting temperature by 4.3 °C maximally at a concentration of 5 mM, with higher concentrations resulting in more modest increases similar to those obtained for much lower concentrations of Mg^{2+} (Figure S3 of the Supporting Information). Surprisingly, titration of APE1 with E3330 decreased the melting temperature in a concentration-dependent manner. E3330 was added to a maximal concentration of 1 mM dissolved in either 2% ethanol (data not shown), as used in the NMR study,[30] or 2% DMSO,

dx.doi.org/10.1021/bi400179m | *Biochemistry* 2013, 52, 2955−2966

as used in our previous studies and in the HDX study discussed above. In both cases, the melting temperature of APE1 decreased by 5 °C for the 1 mM E3330 sample (Figure 3). The same experiment was repeated in the presence of 1 mM Mg^{2+}, which increases the melting temperature by ~3 °C, with similar results. Although the starting T_m was higher for E3330 and Mg^{2+}, the melting temperature when 1 mM E3330 was added decreased by 4.4 °C (Figure 3).

To confirm the results obtained using DSF, we employed circular dichroism to determine the melting temperature of full-length APE1 in the presence and absence of E3330. In reasonable agreement with the DSF experiments, the melting temperature of APE1 was 46 °C (Figure 4A). As noted in

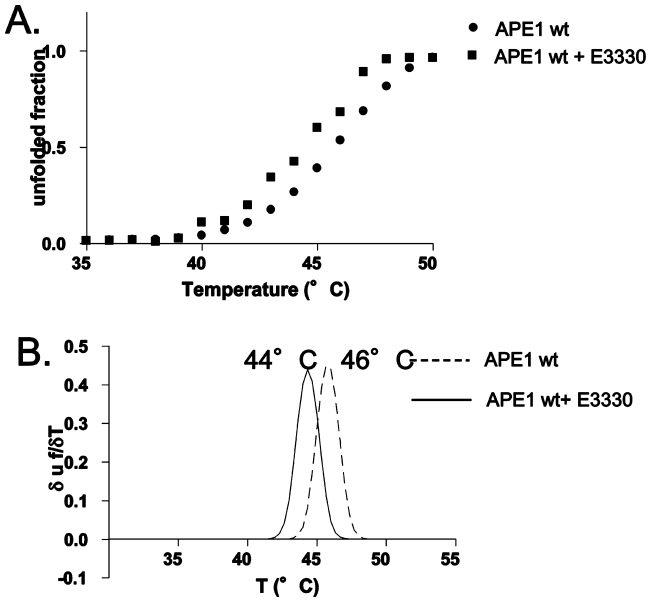

Figure 4. Effect of E3330 on APE1's melting temperature as measured by CD. (A) Overlay of thermal melting profiles of recombinant APE1 with and without E3330, reported as unfolded fraction vs temperature, as measured through the CD signal at 230 nm. (B) First derivative of denaturation sigmoidal curves.

Experimental Procedures, the CD experiments were performed in 10 mM phosphate buffer (pH 7.0) to diminish the contributions of absorbance from organic buffers. Because of the interference in the CD spectrum by DMSO, the solvent used to solubilize E3330, it was not possible to conduct this experiment at E3330 concentrations above 0.5 mM. Nevertheless, using an E3330 concentration of 0.5 mM, we found the melting temperature of APE1 decreased by 2 °C (Figure 4B). The decrease in melting temperature obtained by DSF was also 2 °C for addition of 0.5 mM E3330. Therefore, the results obtained by both DSF and CD methods are entirely consistent.

Thus, rather than stabilizing the structure of APE1 as previously suggested,[30] addition of E3330 results in destabilization or loss of structure as indicated by the lowered melting temperature. We proposed earlier that the binding of E3330 stabilizes a partially unfolded form of APE1, not its low-energy fully folded structure, and the results thus far are consistent with this hypothesis. That is, both NMR and HDX by MS show that an interaction occurs, and melting-point depression shows that the interaction is destabilizing.

Inhibition of APE1's Redox Activity by E3330 and E3330-amide. We previously demonstrated that E3330 blocked the redox signaling function of APE1 with AP-1, HIF-1α, NF-κB, and other downstream transcription factors as the targets *in vitro* and *in vivo*.[26,29,33,35,42] However, we had not established in these studies whether the negatively charged carboxylate of E3330 was required for redox inhibition. Thus, we synthesized a methoxy amide derivative of E3330, (*E*)-2-[(4,5-dimethoxy-2-methyl-3,6-dioxocyclohexa-1,4-dien-1-yl)-methylene]-*N*-methoxy-undecanamide (E3330-amide) (Scheme 1). The methoxy amide potentially affords improved solubility as compared to the comparable methyl amide or unsubstituted amide derivatives. We then compared the ability of E3330 and E3330-amide, an uncharged derivative of E3330 (Scheme 1), to inhibit the redox activity of APE1 by using a standard redox EMSA. In this assay, oxidized c-Jun must be reduced by APE1, resulting in reduced c-Jun that binds DNA and yields a shifted band by EMSA analysis. As demonstrated in Figure 5A, E3330-amide inhibited AP-1-enhanced DNA binding by APE1 in a dose-dependent manner similar to that observed for E3330, albeit with a lower IC_{50} of 8.5 μM compared to the value of 20 μM for E3330. Subsequent analyses in the cell-based NF-κB luciferase reporter assay performed in Panc1 cells treated with E3330 or E3330-amide resulted in a significant decrease in NF-κB activity. Similar to AP-1, NF-κB is also a target of APE1 redox signaling. In this redox transactivation analysis, E3330 had a higher IC_{50} (55 μM) than E3330-amide (7 μM) (Figure 5B). These results indicate that E3330-amide is an effective redox inhibitor of APE1, as revealed by using both an *in vitro* redox EMSA and a cell-based redox target transactivation assay. Previous studies have demonstrated that APE1 plays an important role in cell growth and survival through two main functions: DNA repair AP endonuclease activity and redox signaling function.[1,2,10,26,27,29,33,43−50] Inhibition of the redox activity of APE1 by E3330 also prevented tumor cell growth as a cytostatic agent.[35,48,49] Not surprisingly, E3330-amide also blocked the growth of ovarian cancer cell line SKOV-3X (Figure 5C). The effect was more pronounced with an LD_{50} of 54 μM compared to that of E3330 (LD_{50} = 104 μM) in these studies. Thus, E3330-amide has cell killing capabilities in cancer cells, similar to if not better than those of E3330.

Effect of E3330 and E3330-amide on APE1 AP Endonuclease Activity. We and others have demonstrated that E3330 blocks the redox function of APE1 but does not inhibit the apurinic/apyrimidinic (AP) endonuclease activity of APE1 at concentrations lower than 100 μM.[23,29,33,35] To determine whether E3330-amide inhibits the endonuclease function of APE1, we used two different assays: a gel-based and a high-throughput screening (HTS) plate-based assay.[38,51] The previously reported analyses were performed by using concentrations of E3330 that inhibited the redox function of APE1 at time points of <30 min. To confirm these previous findings and to ascertain the effect of E3330-amide on APE1 endonuclease activity, we tested inhibition at longer times and higher concentrations. In the gel-based assay (Figure 6A), E3330 did not show any inhibition of APE1 repair activity when reacted with APE1 from 30 min to 2 h below concentrations of 160 μM. Similarly, in an HTS assay, neither E3330 nor E3330-amide had a significant effect on APE1 repair activity up to 100 μM (Figure 6B,C); APE1 retained at least 85% activity.

Effect of E3330-amide on the Melting Temperature of APE1. We performed DSF assays using the uncharged derivative E3330-amide to determine whether the negatively

dx.doi.org/10.1021/bi400179m | *Biochemistry* 2013, 52, 2955−2966

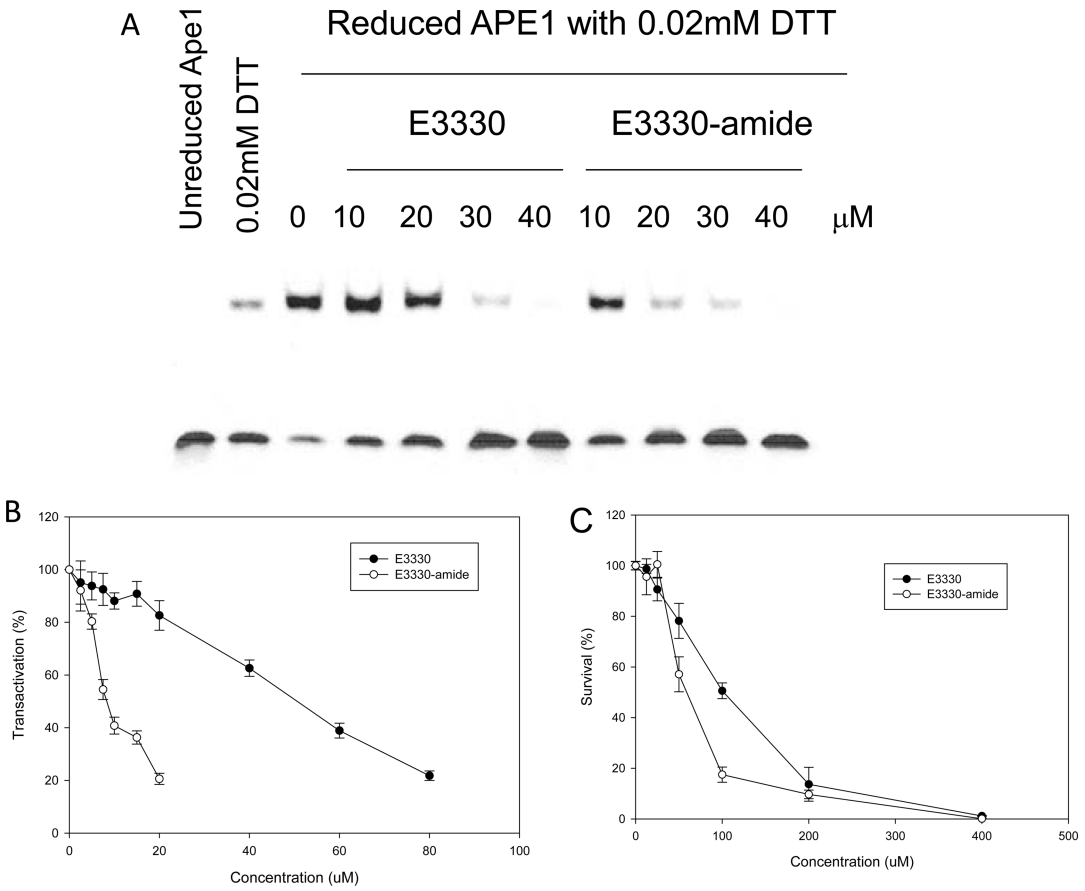

Figure 5. Inhibition of APE1's redox activity by E3330 and E3330-amide. (A) Redox EMSA. E3330 or its derivative E3330-amide was incubated with 2 μL of purified APE1 (reduced with 1.0 mM DTT for 10 min and then diluted to a concentration of 0.06 mM with 0.2 mM DTT in PBS) in EMSA reaction buffer in a total volume of 16 μL for 30 min, and then the EMSA was performed. Final concentrations of APE1 and DTT were 0.006 and 0.02 mM, respectively. Controls included reactions with unreduced APE1 and with 0.02 mM DTT, which is carried over in the reduced APE1 samples. E3330-amide inhibited AP-1 DNA binding enhanced by APE1 in dose-dependent manner as did E3330, albeit at a lower IC_{50} of 8.5 μM vs an IC_{50} of 20 μM for E3330. (B) Transactivation assay. E3330 or E3330-amide was added to the Panc1 stable cells with the pGreenFire-NF-κB gene. After treatment had been conducted for 40 h, NF-κB-stimulated luciferase activity was measured along with a MTT assay to measure the cell number. The ratio of luciferase activity to MTT activity was determined as a measure of NF-κB activity. Data are expressed as means ± the standard error of the mean (SEM) of three independent experiments performed in duplicate and are shown as a percentage of transactivation compared with control without E3330 or E3330-amide. E3330-amide had a greater effect on NF-κB transactivation with an IC_{50} of 7 μM compared to an IC_{50} of 55 μM for E3330. (C) Effect of E3330 and E3330-amide on cell growth and survival in an ovarian cancer cell line. The MTT assay was used to measure the effect of E3330 and E3330-amide on cell growth and survival. Data are expressed as the means ± SEM of three independent experiments performed in triplicate. E3330-amide caused a decrease in the amount of cell proliferation in dose-dependent manner and was more effective than E3330.

charged carboxylate moiety is required for interaction with APE1 in its folded state. In contrast to E3330, no concentration-dependent change in melting temperature was observed for E3330-amide (Figure 7) in the presence or absence of 1 mM Mg^{2+}. Observed differences in melting temperature were ≤1 °C for different concentrations of E3330-amide. Thus, E3330-amide does not appear to interact with APE1 in its folded state, yet it is a more effective redox inhibitor than E3330.

DISCUSSION

Results presented here provide new insights into the mechanism by which E3330 interacts with and inhibits the redox activity of APE1. By using HDX mass spectrometry, we identified two sites of interaction for E3330 that are proximal to the repair active site (Figure 2B). Although these data are consistent with an interaction of E3330 and the repair active site of APE1, the fact that there is no evidence of E3330-amide interacting with the repair active site of APE1 suggests a role for the negatively charged carboxylate in the interaction. There are a number of positively charged residues lining the DNA-binding site of APE1, including R177 and R73, both of which are solvent-exposed and would provide favorable electrostatic interactions (Figure 2B) with E3330, localizing it to the regions observed in the HDX experiment to be E3330-interacting. This lack of singular specificity is in accord with the relatively large K_d of 390 μM.[30]

The effect of the interaction of E3330 with APE1 is a decrease in its melting temperature as measured by DSF and CD. These results suggest that E3330 destabilizes APE1's structure rather than stabilizing it. Previously, we proposed that even at room temperature APE1 can adopt a partially unfolded state. This idea is supported by APE1's relatively low melting temperature determined by both DSF and CD (46 °C) in these studies. We further proposed that the partially unfolded state of APE1 is stabilized through interaction with E3330. In this

dx.doi.org/10.1021/bi400179m | *Biochemistry* 2013, 52, 2955−2966

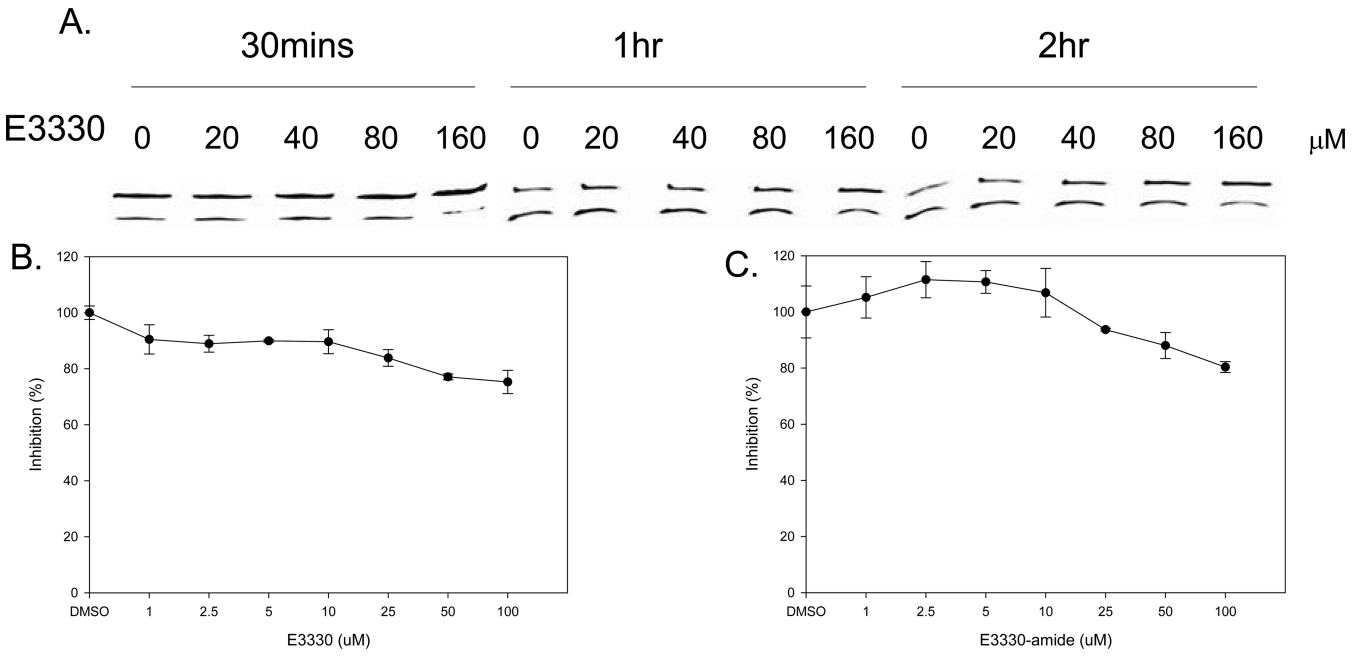

Figure 6. Inhibition of APE1's endonuclease activity by E3330 and E3330-amide. (A) Oligonucleotide gel-based APE1 endonuclease activity assays. Oligonucleotide gel-based APE1 endonuclease activity assays were performed as described in Experimental Procedures. The top band (26-mer) represents uncleaved AP oligonucleotide, whereas the bottom band (14-mer) is the cleaved oligonucleotide. No inhibition of APE1's endonuclease activity was observed for E3330 concentrations of <160 μM. (B and C) HTS assay for the inhibition of APE1 endonuclease DNA repair activity. When testing for APE1 DNA repair inhibition, we found the addition of up to 100 μM E3330 (B) or E3330-amide (C) did not result in a decrease in the reaction rate, an indicator of the lack of inhibition.

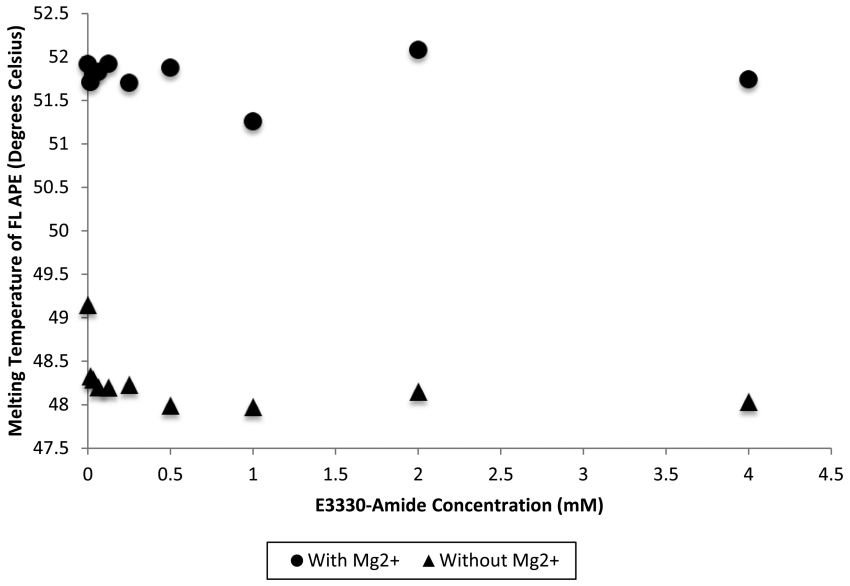

Figure 7. Effect of E3330-amide on APE1's melting temperature as measured by DSF. APE1 was titrated with increasing concentrations of E3330-amide dissolved in DMSO (16 μM to 4 mM) in the presence and absence of 1 mM Mg^{2+}. SYPRO orange dye was then added, and T_m measurements were taken by DSF. The resulting T_m of APE1 was plotted vs the concentration of E3330-amide in the presence or absence of 1 mM Mg^{2+}. Increasing concentrations of E3330-amide did not produce a change in the T_m of APE1.

partially unfolded state, APE1 is susceptible to reaction with NEM, resulting in labeling of all seven of its Cys residues.[29] In the absence of E3330, only the two solvent-accessible Cys residues are labeled with NEM.[29] Thus, our results strengthen the conclusion from our previous studies.[29] Inclusion of Mg^{2+} increases the melting temperature of APE1, consistent with stabilization of the structure. However, addition of E3330 even in the presence of Mg^{2+} results in a decrease in the melting temperature, suggesting that there is no stabilization of APE1's structure through interaction of the carboxylate group of E3330 and Mg^{2+}, as might have been expected if the compound binds as modeled in the repair active site pocket.[30] Our results do not support the proposal that E3330 acts as a redox inhibitor by binding specifically to the repair active site of APE1 and preventing the enzyme from adopting an alternate conformation.[30] We further note that inhibition of APE1's endonuclease activity by E3330 at relatively high concentrations is consistent

dx.doi.org/10.1021/bi400179m | *Biochemistry* 2013, 52, 2955−2966

with destabilization of APE1's structure observed by DSF and CD at similarly high concentrations.

The next question is whether the carboxylate of E3330 is required for inhibition of APE1's redox activity. E3330-amide was found to be a more effective redox inhibitor than E3330 in *in vitro* redox, cell-based transactivation, and cell-killing assays. Thus, the carboxylate of E3330 is not essential for redox inhibition. In contrast to E3330, E3330-amide does not affect the melting temperature of APE1, suggesting that it does not interact directly with folded APE1. Given that it is a more effective redox inhibitor, we envision the following scenario. Similar to E3330, E3330-amide likely interacts with the redox active form of APE1, which has been proposed to be a locally unfolded state of the protein.[29] However, because it lacks the negatively charged carboxylate, E3330-amide has a much lower affinity than E3330 for the positively charged repair active site of the fully folded enzyme.

In conclusion, what emerges from this study and previous work is that E3330 is an effective redox inhibitor but is a poor endonuclease inhibitor with *in vitro* concentrations of >100 μM required for inhibition. E3330 contrasts with a large number of negatively charged endonuclease inhibitors with IC_{50} values in the range of 0.1−10 μM[38,51−54] and would not have been identified in an experimental screen as an endonuclease inhibitor as most screens are performed using small molecules at concentrations of 10−20 μM. However, at high concentrations, E3330 does interact with the repair active site, albeit without complete specificity, and with low affinity that depends on its negatively charged carboxylate group. We suggest that the properties that make E3330 and its amide derivative effective redox inhibitors are its quinone group, important for inhibiting the redox reaction,[35,42] and its hydrophobic character, allowing it to interact with APE1 in a partially unfolded state.[29]

■ ASSOCIATED CONTENT

Supporting Information

HDX peptide data for full-length APE1 and full-length APE1−E3330 (1.6 mM) samples, selected HDX peptide data comparing experiments conducted at 25 μM and 1.6 mM E3330, and DSF data for a titration of APE1 with increasing concentrations of Mg^{2+}. This material is available free of charge via the Internet at http://pubs.acs.org.

■ AUTHOR INFORMATION

Corresponding Author

*Department of Biochemistry and Molecular Biology, 635 Barnhill Dr., MS 4032, Indianapolis, IN 46202. E-mail: mgeorgia@iu.edu. Phone: (317) 278-8486. Fax: (317) 274-4686.

Funding

This work was supported by National Institutes of Health (NIH) Grant CA114571 to M.M.G., NIH Grants CA121168, CA114571, and CA121168S1 and a Riley Children's Foundation grant to M.R.K., and NIH Grant 8 P41 GM103422 to M.L.G.

Notes

The authors declare no competing financial interest.

■ ACKNOWLEDGMENTS

We thank Jim Wikel for assistance in designing redox inhibitors, Sandor Vajda and his laboratory at Boston University (Boston, MA) for assistance in docking of E3330 in the repair active site of APE1, Bruce Pascal from Professor Patrick R. Griffin's laboratory at Scripps Florida (Jupiter, FL) for help with HDX data analysis and helpful discussion, Halesha Basavarajappa and Krishna Mahalingan for assistance with earlier studies related to this work, and members of the Georgiadis and Kelley laboratories for helpful discussion related to the manuscript.

■ REFERENCES

(1) Luo, M., He, H., Kelley, M. R., and Georgiadis, M. M. (2010) Redox regulation of DNA repair: Implications for human health and cancer therapeutic development. *Antioxid. Redox Signaling 12*, 1247−1269.

(2) Tell, G., Quadrifoglio, F., Tiribelli, C., and Kelley, M. R. (2009) The Many Functions of APE1/Ref-1: Not Only a DNA Repair Enzyme. *Antioxid. Redox Signaling 11*, 601−620.

(3) Koukourakis, M. I., Giatromanolaki, A., Kakolyris, S., Sivridis, E., Georgoulias, V., Funtzilas, G., Hickson, I. D., Gatter, K. C., and Harris, A. L. (2001) Nuclear expression of human apurinic/apyrimidinic endonuclease (HAP1/Ref-1) in head-and-neck cancer is associated with resistance to chemoradiotherapy and poor outcome. *Int. J. Radiat. Oncol., Biol., Phys. 50*, 27−36.

(4) Kakolyris, S., Kaklamanis, L., Engels, K., Fox, S. B., Taylor, M., Hickson, I. D., Gatter, K. C., and Harris, A. L. (1998) Human AP endonuclease 1 (HAP1) protein expression in breast cancer correlates with lymph node status and angiogenesis. *Br. J. Cancer 77*, 1169−1173.

(5) Robertson, K. A., Bullock, H. A., Xu, Y., Tritt, R., Zimmerman, E., Ulbright, T. M., Foster, R. S., Einhorn, L. H., and Kelley, M. R. (2001) Altered expression of Ape1/ref-1 in germ cell tumors and overexpression in NT2 cells confers resistance to bleomycin and radiation. *Cancer Res. 61*, 2220−2225.

(6) Fung, H., and Demple, B. (2005) A vital role for Ape1/Ref1 protein in repairing spontaneous DNA damage in human cells. *Mol. Cell 17*, 463−470.

(7) Tell, G., Crivellato, E., Pines, A., Paron, I., Pucillo, C., Manzini, G., Bandiera, A., Kelley, M. R., Di Loreto, C., and Damante, G. (2001) Mitochondrial localization of APE/Ref-1 in thyroid cells. *Mutat. Res. 485*, 143−152.

(8) Chattopadhyay, R., Wiederhold, L., Szczesny, B., Boldogh, I., Hazra, T. K., Izumi, T., and Mitra, S. (2006) Identification and characterization of mitochondrial abasic (AP)-endonuclease in mammalian cells. *Nucleic Acids Res. 34*, 2067−2076.

(9) Tell, G., and Wilson, D. M., III (2010) Targeting DNA repair proteins for cancer treatment. *Cell. Mol. Life Sci. 67*, 3569−3572.

(10) Kelley, M., Georgiadis, M., and Fishel, M. (2012) APE1/Ref-1 Role in Redox Signaling: Translational Applications of Targeting the Redox Function of the DNA Repair/Redox Protein APE1/Ref-1. *Curr. Mol. Pharmacol. 5*, 36−53.

(11) Demple, B., Herman, T., and Chen, D. S. (1991) Cloning and expression of APE, the cDNA encoding the major human apurinic endonuclease: Definition of a family of DNA repair enzymes. *Proc. Natl. Acad. Sci. U.S.A. 88*, 11450−11454.

(12) Xanthoudakis, S., and Curran, T. (1992) Identification and characterization of Ref-1, a nuclear protein that facilitates AP-1 DNA-binding activity. *EMBO J. 11*, 653−665.

(13) Bhakat, K. K., Yang, S. H., and Mitra, S. (2003) Acetylation of human AP-endonuclease 1, a critical enzyme in DNA repair and transcription regulation. *Methods Enzymol. 371*, 292−300.

(14) Vascotto, C., Fantini, D., Romanello, M., Cesaratto, L., Deganuto, M., Leonardi, A., Radicella, J. P., Kelley, M. R., D'Ambrosio, C., Scaloni, A., Quadrifoglio, F., and Tell, G. (2009) APE1/Ref-1 interacts with NPM1 within nucleoli and plays a role in the rRNA quality control process. *Mol. Cell. Biol. 29*, 1834−1854.

(15) Hirota, K., Matsui, M., Iwata, S., Nishiyama, A., Mori, K., and Yodoi, J. (1997) AP-1 transcriptional activity is regulated by a direct association between thioredoxin and Ref-1. *Proc. Natl. Acad. Sci. U.S.A. 94*, 3633−3638.

(16) Wei, S. J., Botero, A., Hirota, K., Bradbury, C. M., Markovina, S., Laszlo, A., Spitz, D. R., Goswami, P. C., Yodoi, J., and Gius, D. (2000) Thioredoxin nuclear translocation and interaction with redox factor-1 activates the activator protein-1 transcription factor in response to ionizing radiation. *Cancer Res. 60*, 6688−6695.
(17) Ziel, K. A., Campbell, C. C., Wilson, G. L., and Gillespie, M. N. (2004) Ref-1/Ape is critical for formation of the hypoxia-inducible transcriptional complex on the hypoxic resonse element of the rat pulmonary artery endothelial cell VEGF. *FASEB J. 18*, 986−988.
(18) Gray, M. J., Zhang, J., Ellis, L. M., Semenza, G. L., Evans, D. B., Watowich, S. S., and Gallick, G. E. (2005) HIF-1α, STAT3, CBP/p300 and Ref-1/APE are components of a transcriptional complex that regulates Src-dependent hypoxia-induced expression of VEGF in pancreatic and prostate carcinomas. *Oncogene 24*, 3110−3120.
(19) Pines, A., Perrone, L., Bivi, N., Romanello, M., Damante, G., Gulisano, M., Kelley, M. R., Quadrifoglio, F., and Tell, G. (2005) Activation of APE1/Ref-1 is dependent on reactive oxygen species generated after purinergic receptor stimulation by ATP. *Nucleic Acids Res. 33*, 4379−4394.
(20) Pines, A., Bivi, N., Romanello, M., Damante, G., Kelley, M. R., Adamson, E. D., D'Andrea, P., Quadrifoglio, F., Moro, L., and Tell, G. (2005) Cross-regulation between Egr-1 and APE/Ref-1 during early response to oxidative stress in the human osteoblastic HOBIT cell line: Evidence for an autoregulatory loop. *Free Radical Res. 39*, 269−281.
(21) Jayaraman, L., Murthy, K. G., Zhu, C., Curran, T., Xanthoudakis, S., and Prives, C. (1997) Identification of redox/repair protein Ref-1 as a potent activator of p53. *Genes Dev. 11*, 558−570.
(22) Madhusudan, S., and Hickson, I. D. (2005) DNA repair inhibition: A selective tumour targeting strategy. *Trends Mol. Med. 11*, 503−511.
(23) Luo, M., Zhang, J., He, H., Su, D., Chen, Q., Gross, M. L., Kelley, M. R., and Georgiadis, M. M. (2012) Characterization of the redox activity and disulfide bond formation in apurinic/apyrimidinic endonuclease. *Biochemistry 51*, 695−705.
(24) Kim, Y. J., Kim, D., Illuzzi, J. L., Delaplane, S., Su, D., Bernier, M., Gross, M. L., Georgiadis, M. M., and Wilson, D. M., III (2011) S-Glutathionylation of cysteine 99 in the APE1 protein impairs abasic endonuclease activity. *J. Mol. Biol. 414*, 313−326.
(25) Walker, L. J., Robson, C. N., Black, E., Gillespie, D., and Hickson, I. D. (1993) Identification of residues in the human DNA repair enzyme HAP1 (Ref-1) that are essential for redox regulation of Jun DNA binding. *Mol. Cell. Biol. 13*, 5370−5376.
(26) Georgiadis, M., Luo, M., Gaur, R., Delaplane, S., Li, X., and Kelley, M. (2008) Evolution of the redox function in mammalian apurinic/apyrimidinic endonuclease. *Mutat. Res. 643*, 54−63.
(27) Vascotto, C., Bisetto, E., Li, M., Zeef, L. A., D'Ambrosio, C., Domenis, R., Comelli, M., Delneri, D., Scaloni, A., Altieri, F., Mavelli, I., Quadrifoglio, F., Kelley, M. R., and Tell, G. (2011) Knock-in reconstitution studies reveal an unexpected role of Cys-65 in regulating APE1/Ref-1 subcellular trafficking and function. *Mol. Biol. Cell 22*, 3887−3901.
(28) Shimizu, N., Sugimoto, K., Tang, J., Nishi, T., Sato, I., Hiramoto, M., Aizawa, S., Hatakeyama, M., Ohba, R., Hatori, H., Yoshikawa, T., Suzuki, F., Oomori, A., Tanaka, H., Kawaguchi, H., Watanabe, H., and Handa, H. (2000) High-performance affinity beads for identifying drug receptors. *Nat. Biotechnol. 18*, 877−881.
(29) Su, D., Delaplane, S., Luo, M., Rempel, D. L., Vu, B., Kelley, M. R., Gross, M. L., and Georgiadis, M. M. (2011) Interactions of Apurinic/Apyrimidinic Endonuclease with a Redox Inhibitor: Evidence for an Alternate Conformation of the Enzyme. *Biochemistry 50*, 82−92.
(30) Manvilla, B. A., Wauchope, O., Seley-Radtke, K. L., and Drohat, A. C. (2011) NMR studies reveal an unexpected binding site for a redox inhibitor of AP endonuclease 1. *Biochemistry 50*, 10540−10549.
(31) Li, M., Zhong, Z., Zhu, J., Xiang, D., Dai, N., Cao, X., Qing, Y., Yang, Z., Xie, J., Li, Z., Baugh, L., Wang, G., and Wang, D. (2010) Identification and characterization of mitochondrial targeting sequence of human apurinic/apyrimidinic endonuclease 1. *J. Biol. Chem. 285*, 14871−14881.
(32) Zhang, J., Chalmers, M. J., Stayrook, K. R., Burris, L. L., Garcia-Ordonez, R. D., Pascal, B. D., Burris, T. P., Dodge, J. A., and Griffin, P. R. (2010) Hydrogen/deuterium exchange reveals distinct agonist/partial agonist receptor dynamics within vitamin D receptor/retinoid X receptor heterodimer. *Structure 18*, 1332−1341.
(33) Luo, M., Delaplane, S., Jiang, A., Reed, A., He, Y., Fishel, M., Nyland, R. L., II, Borch, R. F., Qiao, X., Georgiadis, M. M., and Kelley, M. R. (2008) Role of the multifunctional DNA repair and redox signaling protein Ape1/Ref-1 in cancer and endothelial cells: Small molecule inhibition of Ape1's redox functio. *Antioxid. Redox Signaling 10*, 1853−1867.
(34) Wang, D., Luo, M., and Kelley, M. R. (2004) Human apurinic endonuclease 1 (APE1) expression and prognostic significance in osteosarcoma: Enhanced sensitivity of osteosarcoma to DNA damaging agents using silencing RNA APE1 expression inhibition. *Mol. Cancer Ther. 3*, 679−686.
(35) Kelley, M. R., Luo, M., Reed, A., Su, D., Delaplane, S., Borch, R. F., Nyland, R. L., Gross, M. L., and Georgiadis, M. M. (2011) Functional Analysis of Novel Analogues of E3330 That Block the Redox Signaling Activity of the Multifunctional AP Endonuclease/Redox Signaling Enzyme APE1/Ref-1. *Antioxid. Redox Signaling 14*, 1387−1401.
(36) Kreklau, E. L., Limp-Foster, M., Liu, N., Xu, Y., Kelley, M. R., and Erickson, L. C. (2001) A novel fluorometric oligonucleotide assay to measure O(6)-methylguanine DNA methyltransferase, methylpurine DNA glycosylase, 8-oxoguanine DNA glycosylase and abasic endonuclease activities: DNA repair status in human breast carcinoma cells overexpressing methylpurine DNA glycosylase. *Nucleic Acids Res. 29*, 2558−2566.
(37) Luo, M., and Kelley, M. R. (2004) Inhibition of the human apurinic/apyrimidinic endonuclease (APE1) repair activity and sensitization of breast cancer cells to DNA alkylating agents with lucanthone. *Anticancer Res. 24*, 2127−2134.
(38) Bapat, A., Glass, L. S., Luo, M., Fishel, M. L., Long, E. C., Georgiadis, M. M., and Kelley, M. R. (2010) Novel small molecule inhibitor of Ape1 endonuclease blocks proliferation and reduces viability of glioblastoma cells. *J. Pharmacol. Exp. Ther. 334*, 988−998.
(39) Gorman, M. A., Morera, S., Rothwell, D. G., La Fortelle, E., Mol, C. D., Tainer, J. A., Hickson, I. D., and Freemont, P. S. (1997) The crystal structure of the human DNA repair endonuclease HAP1 suggests the recognition of extra-helical deoxyribose at DNA abasic sites. *EMBO J. 16*, 6548−6558.
(40) Beernink, P. T., Segelke, B. W., Hadi, M. Z., Erzberger, J. P., Wilson, D. M., III, and Rupp, B. (2001) Two divalent metal ions in the active site of a new crystal form of human apurinic/apyrimidinic endonuclease, Ape1: Implications for the catalytic mechanism. *J. Mol. Biol. 307*, 1023−1034.
(41) Niesen, F. H., Berglund, H., and Vedadi, M. (2007) The use of differential scanning fluorimetry to detect ligand interactions that promote protein stability. *Nat. Protoc. 2*, 2212−2221.
(42) Nyland, R. L., Luo, M., Kelley, M. R., and Borch, R. F. (2010) Design and synthesis of novel quinone inhibitors targeted to the redox function of apurinic/apyrimidinic endonuclease 1/redox enhancing factor-1 (Ape1/ref-1). *J. Med. Chem. 53*, 1200−1210.
(43) Jiang, A., Gao, H., Kelley, M. R., and Qiao, X. (2011) Inhibition of APE1/Ref-1 Redox Activity with APX3330 Blocks Retinal Angiogenesis in vitro and in vivo. *Vision Res. 51*, 93−100.
(44) Jedinak, A., Dudhgaonkar, S., Kelley, M. R., and Sliva, D. (2011) Apurinic/Apyrimidinic endonuclease 1 regulates inflammatory response in macrophages. *Anticancer Res. 31*, 379−385.
(45) Jiang, Y., Zhou, S., Sandusky, G. E., Kelley, M. R., and Fishel, M. L. (2010) Reduced expression of DNA repair and redox signaling protein APE1/Ref-1 impairs human pancreatic cancer cell survival, proliferation, and cell cycle progression. *Cancer Invest. 28*, 885−895.
(46) Fishel, M. L., Colvin, E. S., Luo, M., Kelley, M. R., and Robertson, K. A. (2010) Inhibition of the redox function of APE1/Ref-1 in myeloid leukemia cell lines results in a hypersensitive response to retinoic acid-induced differentiation and apoptosis. *Exp. Hematol. 38*, 1178−1188.

(47) Jiang, Y., Guo, C., Fishel, M. L., Wang, Z.-Y., Vasko, M. R., and Kelley, M. R. (2009) Role of APE1 in differentiated neuroblastoma SH-SY5Y cells in response to oxidative stress: Use of APE1 small molecule inhibitors to delineate APE1 functions. *DNA Repair 8*, 1273−1282.
(48) Jiang, Y., Guo, C., Vasko, M. R., and Kelley, M. R. (2008) Implications of Apurinic/Apyrimidinic Endonuclease in Reactive Oxygen Signaling Response after Cisplatin Treatment of Dorsal Root Ganglion Neurons. *Cancer Res. 68*, 6425−6434.
(49) Fishel, M. L., He, Y., Reed, A. M., Chin-Sinex, H., Hutchins, G. D., Mendonca, M. S., and Kelley, M. R. (2008) Knockdown of the DNA repair and redox signaling protein Ape1/Ref-1 blocks ovarian cancer cell and tumor growth. *DNA Repair 7*, 177−186.
(50) Zou, G. M., Luo, M. H., Reed, A., Kelley, M. R., and Yoder, M. C. (2007) Ape1 regulates hematopoietic differentiation of embryonic stem cells through its redox functional domain. *Blood 109*, 1917−1922.
(51) Madhusudan, S., Smart, F., Shrimpton, P., Parsons, J. L., Gardiner, L., Houlbrook, S., Talbot, D. C., Hammonds, T., Freemont, P. A., Sternberg, M. J., Dianov, G. L., and Hickson, I. D. (2005) Isolation of a small molecule inhibitor of DNA base excision repair. *Nucleic Acids Res. 33*, 4711−4724.
(52) Seiple, L. A., Cardellina, J. H., II, Akee, R., and Stivers, J. T. (2008) Potent inhibition of human apurinic/apyrimidinic endonuclease 1 by arylstibonic acids. *Mol. Pharmacol. 73*, 669−677.
(53) Zawahir, Z., Dayam, R., Deng, J., Pereira, C., and Neamati, N. (2009) Pharmacophore guided discovery of small-molecule human apurinic/apyrimidinic endonuclease 1 inhibitors. *J. Med. Chem. 52*, 20−32.
(54) Simeonov, A., Kulkarni, A., Dorjsuren, D., Jadhav, A., Shen, M., McNeill, D. R., Austin, C. P., and Wilson, D. M., III (2009) Identification and characterization of inhibitors of human apurinic/apyrimidinic endonuclease APE1. *PLoS One 4*, e5740.